Mutagenesis, 2017, 32, 23–31
doi:10.1093/mutage/gew035
Original Manuscript
Advance Access publication 28 July 2016

OXFORD

Original Manuscript

Genotoxic and inflammatory effects of nanofibrillated cellulose in murine lungs

Julia Catalán[1,2,*], Elina Rydman[1], Kukka Aimonen[1], Kati-Susanna Hannukainen[1], Satu Suhonen[1], Esa Vanhala[1], Carlos Moreno[2], Valérie Meyer[3], Denilson da Silva Perez[4], Asko Sneck[5], Ulla Forsström[5], Casper Højgaard[6], Martin Willemoes[6], Jacob R. Winther[6], Ulla Vogel[7], Henrik Wolff[1], Harri Alenius[1], Kai M. Savolainen[1] and Hannu Norppa[1]

[1]Finnish Institute of Occupational Health, P.O. Box 40, FI-00251 Helsinki, Finland, [2]Department of Anatomy, Embryology and Genetics, University of Zaragoza, Miguel Servet 177, 50.013 Zaragoza, Spain, [3]Centre Technique du Papier, CS90251, 38044 Grenoble Cedex 9, France, [4]Institut Technologique FCBA, CS90251, 38044 Grenoble Cedex 9, France, [5]VTT Technical Research Centre of Finland Ltd, P.O. Box 1000, FI-02044 VTT, Finland, [6]Department of Biology, Linderstrøm-Lang Center for Protein Science, University of Copenhagen, Ole Maaloes Vej 5, DK-2200 Copenhagen N, Denmark and [7]National Research Centre for the Working Environment, Lerso Parkallé 105, DK-2100 Copenhagen O, Denmark

*To whom correspondence should be addressed. Tel: +358 43 8251541; Fax: +358304742779; Email: julia.catalan@ttl.fi

Received 27 April 2016; Revised 29 June 2016; Accepted 1 July 2016.

Abstract

Nanofibrillated cellulose (NFC) is a sustainable and renewable nanomaterial, with diverse potential applications in the paper and medical industries. As NFC consists of long fibres of high aspect ratio, we examined here whether TEMPO-(2,2,6,6-tetramethyl-piperidin-1-oxyl) oxidised NFC (length 300–1000 nm, thickness 10–25 nm), administrated by a single pharyngeal aspiration, could be genotoxic to mice, locally in the lungs or systemically in the bone marrow. Female C57Bl/6 mice were treated with four different doses of NFC (10, 40, 80 and 200 μg/mouse), and samples were collected 24 h later. DNA damage was assessed by the comet assay in bronchoalveolar lavage (BAL) and lung cells, and chromosome damage by the bone marrow erythrocyte micronucleus assay. Inflammation was evaluated by BAL cell counts and analysis of cytokines and histopathological alterations in the lungs. A significant induction of DNA damage was observed at the two lower doses of NFC in lung cells, whereas no increase was seen in BAL cells. No effect was detected in the bone marrow micronucleus assay, either. NFC increased the recruitment of inflammatory cells to the lungs, together with a dose-dependent increase in mRNA expression of tumour necrosis factor α, interleukins 1β and 6, and chemokine (C-X-C motif) ligand 5, although there was no effect on the levels of the respective proteins. The histological analysis showed a dose-related accumulation of NFC in the bronchi, the alveoli and some in the cytoplasm of macrophages. In addition, neutrophilic accumulation in the alveolar lung space was observed with increasing dose. Our findings showed that NFC administered by pharyngeal aspiration caused an acute inflammatory response and DNA damage in the lungs, but no systemic genotoxic effect in the bone marrow. The present experimental design did not, however, allow us to determine whether the responses were transient or could persist for a longer time.

Introduction

Nanocellulose is an innovative raw material with diverse potential applications including high quality paper, coatings, food, nanocomposite formulation and reinforcement, and biomedical applications such as drug delivery carriers, cell culture support, substitute implants, tissue repair and regeneration, and antimicrobial materials (1–3). Because nanocelluloses are prepared directly from cellulosic fibres, they are considered genuinely sustainable and renewable materials (4). Nanocelluloses are generally classified into three main groups based on the source and dimensions of the material: nanofibrillated cellulose (NFC, also called microfibrillated cellulose or cellulose nanofibrils), cellulose nanocrystals (CNC, also referred to as nanocrystalline cellulose or cellulose nanowhiskers) and bacterial cellulose (BC, also called microbial cellulose). Nanocellulose dimensions are mainly a consequence of the processing method used to obtain the material (2,5).

NFC consists of aggregates of cellulose microfibrils obtained by the mechanical disintegration of cellulosic materials without the use of hydrolysis, resulting in a low concentrated, viscous and shear thinning aqueous gel which has the ability to form a transparent film, once dried. The key properties of NFC are linked to its high specific area and its extensive hydrogen-bonding ability, allowing its use in nanocomposites, electronics and biomedical applications (6). The production of NFC on an industrial scale may lead to increased exposure to these materials both at workplaces and in the general environment. As NFC consists of long fibres of high aspect ratio, inhaled NFC may have similar properties as nano- and microscale mineral fibres which are known occupational hazards (7–9).

Exposure to cotton or wood dusts, which principally consist of cellulose, can cause respiratory problems and cancer (10,11). Sarcoma formation was described in rats treated intraperitoneally (i.p.) with respirable cellulose fibres (12,13). Several studies using rats or mice suggested that exposure to cellulose fibres by intratracheal administration or inhalation causes inflammation, granulomatous lesions and pulmonary fibrosis (13–17). However, there is very little information on the possible health effects of nanocelluloses. Therefore, the potential adverse effects associated with exposure to NFC and other nanocelluloses need to be assessed.

Knowledge on the toxicity of nanoscale celluloses is still scarce. *In vitro*, low toxic potential to cultured mammalian cells was reported for BC (18–20), CNC (21) and NFC (7,22). These results seemed to be supported by data on the biocompatibility of BC and NFC films, membranes, hydrogels or scaffolds in contact with cultured mammalian cells (23–29). In some *in vitro* studies, cytotoxic effects were described for CNC fibres (30,31). Pharyngeal aspiration of CNC as a gel or a powder facilitated an innate inflammatory response in mice (32,33).

Since nanocelluloses may be inhaled in an aerosolised form during various stages of their life cycle (30), we investigated here whether exposure to NFC by pharyngeal aspiration has genotoxic potential in mice. In addition, inflammatory response, which could be the driving mechanism of possible secondary genotoxicity, was assessed in the same animals.

Materials and methods

NFC production, characterisation and dispersion

NFC was produced, in pilot scale, at the Centre Technique du Papier (Grenoble, France), specifically for this study. In short, spruce sulphite dissolving pulp (Domsjö Fabriker AB, Sweden) was first disintegrated in a slusher and then moved to a TEMPO-oxidation stage, where TEMPO (2,2,6,6-tetramethyl-piperidin-1-oxyl), sodium bromide and sodium hypochlorite were added to the system. The reaction time in the TEMPO-oxidation stage was 2 h. After that, the suspension was washed four times in a centrifuge, to remove the chemical reagents. The washed pulp was then submitted to a mechanical treatment in a high-pressure homogenizer, to ensure the liberation of microfibrils. The resulting suspension was a transparent, gel-like structure of 2% solid content (Figure 1a) to which 50 ppm of the biocide Busan 1009 (Buckmann Laboratories, Ghent, Belgium; containing 10% of 2-(thiocyanomethylthio)benzothiazole, 10% of methylene bis(thiocyanate) and 80% of heavy aromatic naphta and petroleum distillates) was added.

The total acidic group content of the fibres before fibrillation was measured by the conductometric titration method according to the standard SCAN-CM 65:02 (34). The zeta-potential of the NFC particles was determined using Zetasizer Nano ZS equipment (Malvern Instruments Ltd, Malvern, UK). The instrument measures the electrophoretic mobility of particles, which is converted into zeta-potential values using the Smoluchowski model. The measurements were carried out at 25°C in disposable folded capillary cells (Malvern DTS1060) using refractive indices of 1.47 for NFC and 1.33 for the dispersant. The apparent viscosity of the NFC suspension was measured with the Brookfield rheometer RVDV-III Ultra (Brookfield Engineering Laboratories, Middleboro, USA) by using vane geometry at 1.5% solid content. More details of this method are presented by Lahtinen *et al.* (35).

Light microscopic examinations were performed with a Zeiss Axioplan microscope (Carl Zeiss Microscopy GmbH, Göttingen, Germany). To visualise nanoscale fibrils, NFC suspension was deposited on carbon coated grids and then examined with a transmission electron microscope (TEM) (Philips CM200 'Cryo', FEI, Hillsboro, OR, USA), operated at an acceleration voltage of 80 keV.

The 2% water-based stock dispersion of NFC was diluted in phosphate buffered saline (PBS; Lonza, Verviers, Belgium). Dilutions

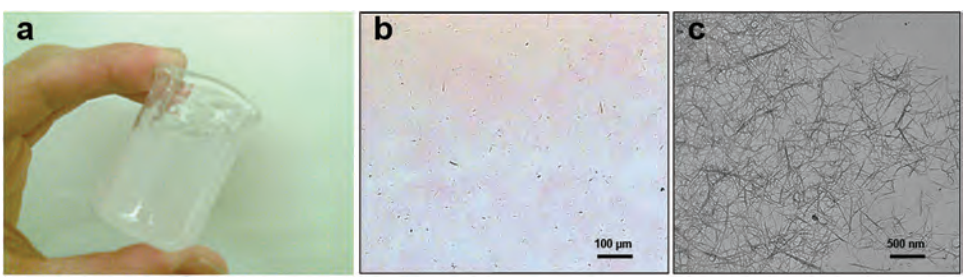

Fig. 1. Macroscopic appearance (**a**), optical microscopy image (**b**) and transmission electron microscope (TEM) micrograph (**c**) illustrating the states of the TEMPO oxidised nanofibrillated cellulose gel.

were sonicated at 37°C for 20 min using a 37 kHz Elmasonic Ultrasound Cleaner (Elmasonic, Singen, Germany), and immediately administrated to the animals by pharyngeal aspiration.

Animals

Female C57Bl/6 mice (7–8 weeks old; ~20 g per mouse) were purchased from Scanbur AB (Sollentuna, Sweden) and quarantined for 1 week. The C57Bl/6 strain was chosen on the basis of the criteria described by Shvedova *et al.* (36) and because methods for the assessment of both genotoxicity and pulmonary inflammation have been developed for this strain. The mice were housed in groups of four, randomly assigned in stainless steel cages bedded with aspen chip, and provided with standard mouse chow diet (Altromin no. 1314 FORTI, Altromin Spezialfutter GmbH & Co., Germany) and tap water *ad libitum*. The environment of the animal room was carefully controlled, with a 12-h dark/light cycle, temperature of 20–21°C and relative humidity of 40–45%. The experiments were performed in agreement with the European Convention for the Protection of Vertebrate Animals Used for Experimental and Other Scientific Purposes (Strasbourg March 18, 1986, adopted in Finland on May 31, 1990). The study was approved by the Animal Experiment Board and the State Provincial Office of Southern Finland.

Pharyngeal aspiration exposure

Pharyngeal aspiration was performed as previously described by Porter *et al.* (37). Eight mice per group were exposed to a single dose (50 µl/mouse) of either PBS alone (negative control group), or 0.2, 0.8, 1.6 or 4 mg/ml of NFC (equivalent to 10, 40, 80 and 200 µg/mouse). The range of doses chosen was similar to the one tested in previous studies with nanocelluloses (32). In addition, a biocide control group received a single dose of 25 ng/mouse of Busan 1009 diluted in PBS, corresponding to the concentration (0.5 ppm) of the biocide present at the highest dose of NFC. Furthermore, a positive control group (n = 6) for the genotoxicity assays was treated with a single 1-mg dose of tungsten carbide-cobalt mixture (WC-Co; a gift from Université catholique de Louvain, Belgium) by pharyngeal aspiration (50 µl/mouse of 20 mg/ml WC-Co in apyrogenic pure water), and with cyclophosphamide (CP; Baxter, Helsinki, Finland) by i.p. injection (50 mg/kg body weight). All mice survived after the exposure and exhibited no negative behavioural or health symptoms. The mice were killed 24 h after the exposure by an overdose of isoflurane, and samples were collected as described below. All the animals were sampled for the immunological and histological analyses, whereas samples for the genotoxicological analyses were collected from six mice per group.

Sample collection

Blood was collected from the *vena cava*, and the lungs were lavaged via the tracheal tube, once with PBS (800 µl for 10 s, at room temperature) for the cytological and immunological analyses of bronchoalveolar lavage (BAL) fluid, and then six times with 0.15 M NaCl (800 µl each, at room temperature) to collect a BAL sample for the comet analyses. The first BAL sample was cytocentrifuged onto a slide, and the cells were stained with May-Grünwald-Giemsa and counted from three high-power fields under a light microscope. The next BAL samples were united and stored on ice (for 2–3 h) until centrifugation (at 400× g for 5 min, 4°C).

The mouse chest was opened, and the right pulmonary lobes were removed, placed onto a petri dish containing 0.15 M NaCl, and then minced and mechanically dispersed to a single cell suspension, as described elsewhere for the comet assay (38). These cells represented a mixture of the different cell types present in the lungs. Half of the left pulmonary lobe was removed, quick-frozen and kept at −70°C for later RNA isolation.

The rest of the lung was formalin-fixed, embedded in paraffin, cut and affixed on slides for histological evaluation. From a few animals, a slice of the lung and BAL cells were fixed with glutaraldehyde and prepared for TEM analyses, as previously described (39).

The femur was dissected from one right back leg and used for bone marrow extraction.

Determination of cytokines and chemokines

RNA isolation from the lung tissues, cDNA synthesis and polymerase chain reaction (PCR) were performed as previously described (40) for analysing the mRNA expression of the pro-inflammatory cytokines interleukins 1β and 6 (IL-1β and IL-6) and tumour necrosis factor α (TNF-α), and the chemokine (C-X-C motif) ligand 5 (CXCL5) in the lung tissue.

To determine the protein levels of the studied cytokines and chemokine, enzyme-linked immunosorbent assay (ELISA) was performed as previously described (40).

Comet assay from BAL and lung suspensions

The comet assay was performed in alkaline conditions (pH > 13) for the BAL and lung cells as previously described (41), in accordance with OECD TG 489 (42). The slides were coded, and one scorer performed the comet analysis using a fluorescence microscope (Axioplan 2, Zeiss, Jena, Germany) and an interactive automated comet counter (Komet 4.0, Kinetic Imaging Ltd., Liverpool, UK). The percentage of DNA in the comet tail was analysed from two slides per animal (50 cells/slide; 100 cells/animal), as recommended by Lovell and Omori (43), to measure the amount of DNA strand breaks.

Automated MN assay in bone marrow erythrocytes

Bone marrow was extracted, and microscopical slides were prepared as previously described (41), in accordance with OECD TG 474 (44). Using the MetaSystems Metafer Metacyte image system (MetaSystems, Altlussheim, Germany) on coded slides, 2000 polychromatic erythrocytes (PCEs) per animal were scored for the frequency of micronucleated polychromatic erythrocytes (MNPCEs) and 1000 erythrocytes per animal to determine the percentages of PCEs and normochromatic erythrocytes (NCEs).

Histological evaluation

The histological preparations were stained with hematoxylin and eosin as previously described (41). In addition, a novel method recently developed for the specific detection of cellulose fibres (9), based on the use of a biotinylated carbohydrate binding module (CBM) of β-1,4-glycanase (EXG:CBM; from *Cellulomonas fimi*), was used. EXG:CBM has been shown to bind quantitatively to various cellulose fibres, including four different NFCs (9). The biotinylated EXG:CBM was visualised by horse radish peroxidase (HRP)-tagged avidin labelling.

Microphotographs were taken with a Leica DM4 B microscope (Immuno Diagnostic Oy LMS, Espoo, Finland) equipped with a 19-mm sCMOS camera imaging port.

Statistical analyses

A hierarchic analysis of variance (ANOVA) was used to study if the percentage of DNA in tail in BAL and lung cells was influenced by the treatments. One-way ANOVA was applied to examine if the

exposures affected the number of different types of cells on the BAL slides, the mRNA and protein expression levels of cytokines and chemokine, and the frequencies of MNPCEs in bone marrow. Dunnett's test was used for an a posteriori comparison of each of the doses with the negative control.

For all end-points analysed, dose–response relationships were investigated by linear regression analysis.

Differences were interpreted to be significant if P was below 0.05. The statistical analyses were performed by the IBM SPSS Statistics for Windows (2013, version 22.0).

Results

Characterisation of NFC

Total acidic group content of the NFC fibres before fibrillation was 1073 µmol/g. After fibrillation, the 2% NFC suspension had a high cellulose surface charge (zeta potential of 69.5 mV), a lightly basic pH (7.98), and conductivity of 730 mS/m. In aqueous environment, the high surface charge of NFC makes it behave like polyelectrolyte rather than typical wood-fibre. The viscosity measurement showed a thixotropic behaviour of the NFC suspension, and the apparent viscosity was 8.6 Pa·s at 1.5% solid content, indicating a gel-like behaviour at low solid content. NFC suspension particle size and shape affected the rheological properties.

Light microscope examinations (Figure 1b) showed a rather homogeneous structure, with only some small residual fibre fragments appearing as dark elements surrounded with NFC which was not visible at this resolution.

The TEM pictures showed well individualised microfibrils having a length range of 300–1000 nm and a thickness range of 10–25 nm (Figure 1c). Therefore, these fibrils had a high aspect ratio (12:1–100:1). Results obtained with the novel fractionation device of the Technical Research Centre of Finland (45) supported the conclusions that this type of NFC with TEMPO pre-treatment contained well individualised microfibrils (over 80% passing 1 µm net), as compared with other NFC samples (produced without TEMPO pre-treatment) with more branched structure.

Immunotoxicity

The degree of pulmonary inflammatory response was estimated by differential counts of alveolar macrophages, neutrophils, eosinophils and lymphocytes in BAL preparations (Figure 2). NFC induced a significant increase in the number of macrophages (P = 0.003) and lymphocytes (P = 0.002) only at the lower two doses (10 and 40 µg/mouse), without showing a linear dose-response. Conversely, a significant increase was observed in neutrophils (P < 0.001) at the highest two doses (80 and 200 µg/mouse) and in eosinophils (P = 0.005) at the highest dose (200 µg/mouse), with a significant linear dose–response (P < 0.005, slope = 0.396 and 0.003, respectively). The biocide (Busan 1009) alone did not affect the number of the inflammatory cells.

NFC induced a significant mRNA expression of the cytokines IL-1β and IL-6 at the highest dose (200 µg/mouse; P = 0.001), showing a significant linear dose–response (P < 0.001, slope = 69.667 and 41.422, respectively) (Figure 3). The mRNA expression of TNF-α was not increased at any of the doses tested in comparison with the negative control group, although there was a significant linear dose-response (P = 0.012, slope = 6.868). The chemokine CXCL5 showed a borderline increase in mRNA expression (P = 0.067) at the highest tested dose (80 µg/mouse in this case), together with a significant linear dose–response (P = 0.002, slope = 45.420). Busan 1009 did not influence the mRNA expression of any of the tested cytokines.

The protein levels of the cytokines and chemokine studied remained unaffected after the NFC or Busan 1009 treatments (data not shown).

Genotoxicity

A significant increase (P < 0.001) in the percentage of DNA in tail, compared with the zero dose, was found in the lung cells at the lowest two doses (10 and 40 µg/mouse) of NFC (Figure 4). However, no effect was observed in BAL cells. NFC did not induce a linear dose–response in any of the cell types. The positive control treatment, WC-Co plus CP, induced a significant increase (P < 0.001) in % DNA in tail for both lung and BAL cells, whereas Busan 1009 showed no effect in either tissue.

NFC did not increase the frequency of MNPCEs in the bone marrow, as shown by the micronucleus assay (Figure 5). Busan 1009 did not either influence the frequency of MNPCEs. On the contrary, the positive control treatment produced a clear response, inducing a 3.4-fold increase in MNPCE frequency (P = 0.005). The percentage of PCEs of all erythrocytes was (average ± SEM) 47.22 ± 1.35, 50.04 ± 5.26, 46.53 ± 2.33, 44.28 ± 1.01, 47.97 ± 1.60, 50.27 ± 3.14 and 44.52 ± 2.41 for the negative control, NFC doses 10, 40, 80 and 200 µg/mouse, biocide and the positive control, respectively. Thus, similar results were obtained with the NFC exposed mice and the unexposed mice, indicating no bone marrow toxicity.

Histology

At necropsy, all animals showed viscera of normal appearance in macroscopic terms. The histological examination of

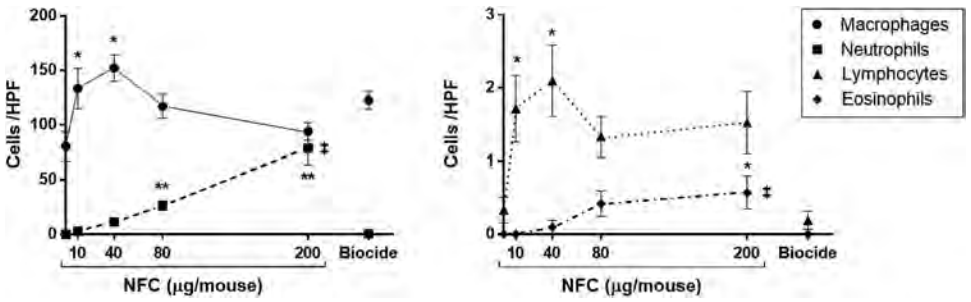

Fig. 2. Cell counts (average ± SEM) from three high-power fields (HPF) of bronchoalveolar lavage (BAL) fluid of mice (eight mice per group) as a function of different doses of a single pharyngeal aspiration with nanofibrillated cellulose (NFC) 24 h post-administration. Asterisks indicate a significant increase (*P < 0.01, **P < 0.001, ANOVA) in comparison with the negative control group, double crosses a significant linear dose-response (P < 0.005, linear regression). BIO, biocide control consisting of Busan 1009 diluted in phosphate-buffered saline at the concentration present at the highest dose of NFC.

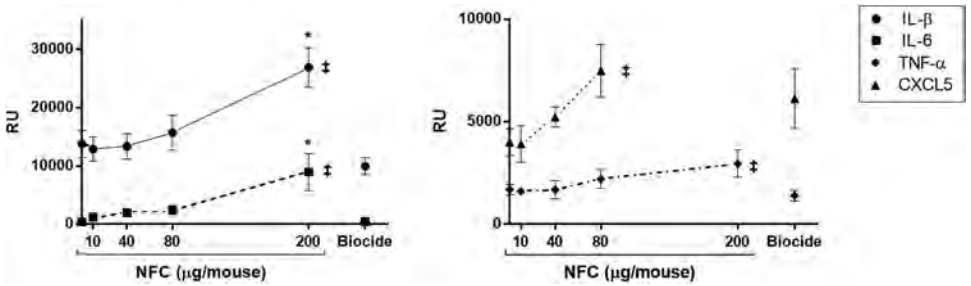

Fig. 3. mRNA expression levels of pro-inflammatory cytokines interleukin 1β (IL-1β) and 6 (IL-6) (LEFT PANEL), and tumour necrosis factor α (TNF- α) and chemokine (C-X-C motif) ligand 5 (CXCL5) (RIGHT PANEL) measured from lung tissues of mice (eight mice per group) 24 h after a single pharyngeal aspiration with different doses of nanofibrillated cellulose (NFC). The results are shown in relative units (RU; average ± SEM). Asterisks indicate a significant increase ($P < 0.01$, ANOVA) in comparison with the negative control group, double crosses a significant linear dose-response ($P < 0.05$, linear regression). BIO, biocide control consisting of Busan 1009 diluted in phosphate buffered saline at the concentration present at the highest dose of NFC.

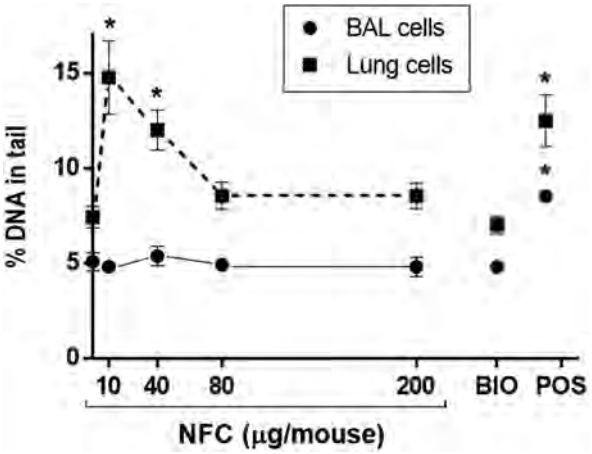

Fig. 4. DNA strand breaks (percentage of DNA in comet tail; average ± SEM) in lung and bronchoalveolar lavage (BAL) cells of mice (six mice per group) 24 h after a single pharyngeal aspiration with different doses of nanofibrillated cellulose (NFC). Asterisks indicate a significant increase ($P < 0.001$, ANOVA) in comparison with the negative control group. BIO, biocide control consisting of Busan 1009 diluted in phosphate buffered saline at the concentration present at the highest dose of NFC; POS, positive control—a combination of tungsten carbide-cobalt mixture (1 mg/mouse, pharyngeal aspiration) and cyclophosphamide (50 mg/kg body weight, intraperitoneally).

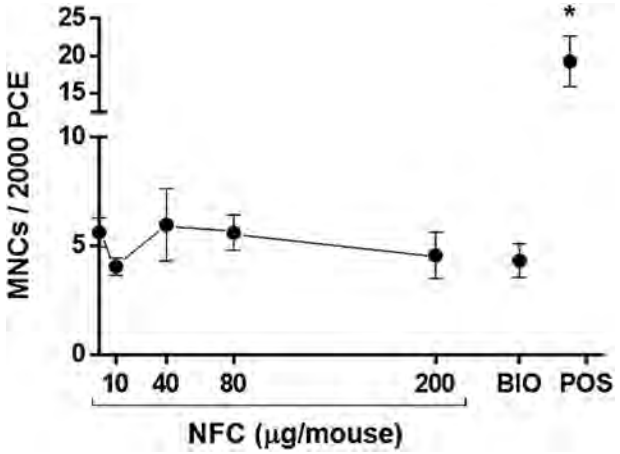

Fig. 5. Frequencies of micronucleated polychromatic erythrocytes (MNPCEs; average ± SEM) among 2000 polychromatic erythrocytes (PCEs) in bone marrow of mice (six mice per group) 24 h after a single pharyngeal aspiration with different doses of nanofibrillated cellulose (NFC). Asterisks indicate a statistically significant difference ($P < 0.01$, ANOVA) in comparison with the negative control group. BIO, biocide control consisting of Busan 1009 diluted in phosphate buffered saline at the concentration present at the highest dose of NFC; POS, positive control consisting of a combination of tungsten carbide-cobalt mixture (1 mg/mouse, pharyngeal aspiration) and cyclophosphamide (50 mg/kg body weight, intraperitoneally).

the lung samples suggested that the accumulation of NFC increased with dose. NFC was found inside the bronchi and in the alveoli (Figure 6a–c). This effect was more clearly seen with the HRP-EXG:CBM staining (Figure 6d and e), which revealed the presence of cellulose material also inside macrophages (Figure 6f). There was a variable and dose-related neutrophilia around the small and large bronchi (Figure 6a–c), as well as neutrophilic accumulation in the alveoli at higher doses. Lung samples from the biocide-treated mice showed a normal appearance, similar to the negative control group (data not shown).

These results were confirmed by TEM analyses which showed the presence of NFC in the alveoli (Figure 7a), recruitment of neutrophils (Figure 7a) and phagocytic activity of macrophages (Figure 7b and c).

Discussion

In this study, the exposure to NFC triggered a recruitment of inflammatory cells to the lungs. Mice exposed to NFC displayed an increase in the number of neutrophils, macrophages, lymphocytes and eosinophils. The overall high level of inflammatory cells upon the NFC exposure indicated an acute inflammatory response. Our results conform with those of Yanamala *et al.* (32) who found that treatment of C57BL/6 mice with two different types of CNCs by pharyngeal aspiration (50–200 µg/mouse) caused increased recruitment of neutrophils, lymphocytes and eosinophils in BAL fluid 24 h post-exposure. In comparison with the negative control, they observed a dose-dependent increase in the percentage of neutrophils and eosinophils but a decrease in the percentage of macrophages. In a recent study, the same authors (33) showed that a repeated cumulative exposure (240 µg/mouse) to CNC caused impaired lung function, pulmonary inflammation and tissue damage 3 months after the last exposure.

Acute cellular responses to airborne particulates are driven by the release of inflammatory mediators. We found a significant dose-dependent increase in the mRNA expression of the four cytokines analysed, although their protein levels remained unaffected. A significant up-regulation of IL-β, IL-6 (32,33) and TNF-α (32), among

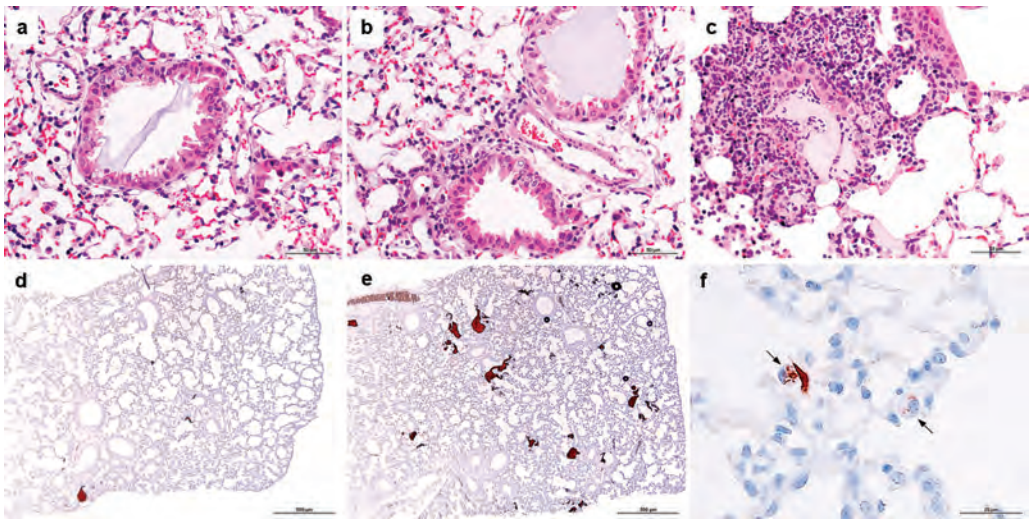

Fig. 6. Mouse lung sections stained with hematoxylin and eosin (**a–c**) and after horse radish peroxidase detection of biotinylated carbohydrate binding module of β-1,4-glycanase (**d–f**), 24 h after a single pharyngeal aspiration with 10 μg/mouse (a, d), 40 μg/mouse (b) or 200 μg/mouse (c, e, f) of nanofibrillated cellulose (NFC). Arrows (f) indicate macrophages containing NFC.

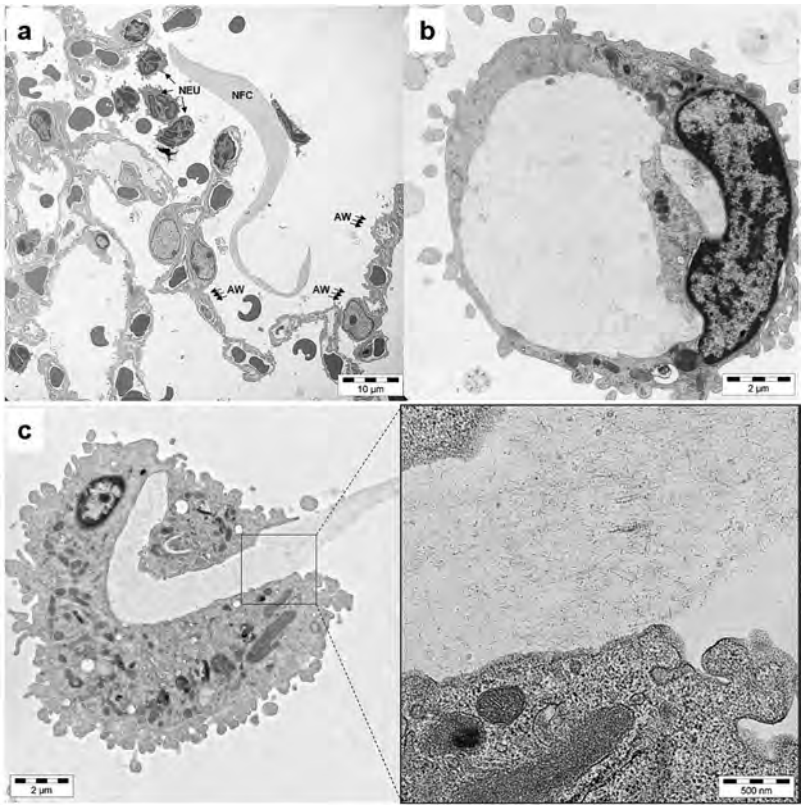

Fig. 7. Transmission electron microscope (TEM) micrographs of mouse lung tissues 24 h after a single pharyngeal aspiration with 80 μg/mouse (**b**) or 200 μg/mouse (**a**, **c**) of nanofibrillated cellulose (NFC). (a) Presence of NFC in the alveolar space with some neutrophils. (b) A bronchoalveolar macrophage full of NFC. (c) A bronchoalveolar macrophage phagocytising NFC. AW, alveolar wall; NEU, neutrophil.

other inflammatory cytokines, was also reported in the BAL fluid of mice after CNC treatments (CXCL5 was not analysed).

Conversely to the *in vivo* studies, nanocelluloses did not seem to be efficient stimulators of the *in vitro* production of cytokines. Colic *et al.* (46) saw no increase in the secretion of IL-1β, TNF-α or Th2 cytokine (IL-4) in NFC-treated (31.25–1000 μg/ml) mouse L929 cells, rat thymocytes or human peripheral blood mononuclear cells. TNF-α expression was neither affected in human acute monocytic leukaemia THP-1 cells treated with 0.4 or 0.8 mg/ml of microfibrillated cellulose (47). Vartiainen *et al.* (7) did not detect increased expression of several cytokines and chemokines, including IL-β, IL-6 and TNF-α, in mouse macrophages or in human monocyte-derived macrophages exposed to microfibrillated cellulose (30–300 μg/ml). CNCs caused no significant stimulation of TNF-α or IL-β in a 3D

triple coculture model of the human epithelial airway barrier (30) or in human monocyte-derived macrophages (31). Whereas all these studies evaluated nanocellulose gels, Hua *et al.* (5) reported a significant secretion of TNF-α and the anti-inflammatory cytokine IL-1 receptor antagonist (IL-1ra) by THP-1 cells in response to NFC films, depending on their different surface chemistries.

NFC induced an increase in DNA damage in the lungs of the mice in the present study. However, this increase was statistically significant only at the lowest two doses, whereas the higher doses exhibited levels of damage similar to the untreated mice. One explanation for this finding might be that, at the higher concentrations, NFC formed larger agglomerates that could more easily be eliminated from the respiratory track by coughing. However, the histological analysis revealed a dose-related accumulation of NFC, with similar distribution inside the bronchi and in the alveoli at all of the doses.

There are only a few studies dealing with the genotoxic potential of nanocelluloses. BC nanofibres did not induce DNA damage in Chinese hamster ovary CHO cells when tested up to 1 mg/ml (19). Similarly, no micronucleus induction was reported in CHO-K1 cells treated with BC membranes (25), in Chinese hamster V79 cells treated with BC/silk fibroin nanocomposites (29), or in BEAS-2B cells treated with CNCs (31). However, de Lima *et al.* (4) reported an induction of DNA strand breaks in Balb/c mouse 3T3 fibroblasts and human peripheral blood lymphocytes as well as chromosomal aberrations in *Allium cepa*, by cellulose nanofibres obtained from curaua and different kinds of cottons, although the genotoxic effect varied depending on the origin of the fibres and the cell type used. Nano-sized cellulose fibrils and BC nanofibres did not increase the number of revertant colonies in the *Salmonella* mutagenicity test (19,22). However, the suitability of this assay for testing nanomaterials has seriously been questioned due to limited uptake of particulates in *Salmonella*; nanomaterials have mostly given negative results in this test (48).

To our knowledge, only one previous study has assessed the genotoxic effects of nanocelluloses *in vivo*. Pinto *et al.* (49) reported no induction of MNPCEs in the bone marrow of Swiss Webster mice treated for 3 days with 200 mg/kg bw/day of BC (dimensions were not described) by oral (gavage) or i.p. administration (sampling 24 h after the last treatment). The mice showed no myelotoxic effects (ratio of PCEs/NCEs) and no clinical signs of toxicity. Moreover, the i.p. BC treatment clearly antagonised the myelotoxic and genotoxic effects of a single i.p. injection of CP (25 mg/kg bw) administrated 45 min after the last BC dose (49). In this study, NFC neither exerted systemic genotoxic effects, as assessed by the micronucleus assay in bone marrow erythrocytes, at doses that induced local DNA damage in the lungs of the same mice. When judging the negative outcome of the micronucleus assay, it should be considered that the 24 h sampling time after the last exposure may have been too short to allow sufficient translocation of nanocellulose to circulation or an adequate secondary genotoxic effect in the bone marrow.

WC-Co, one of the components of our positive control, is another example of a material that has only a local genotoxic effect when administered by pharyngeal aspiration. In our earlier study (41), WC-Co, known to generate reactive oxygen species, induced a significant increase in micronucleated alveolar type II cells in the lungs of the exposed mice but no increase in MNPCEs in the blood. This suggests that the significant elevation of MNPCEs induced by the positive control treatment in the present study was due to the second component, CP, an efficient micronucleus inducer. Our findings again highlight the limitations of the mammalian erythrocyte MN test (44) in testing nanomaterials in short-term studies and the necessity of using and further developing *in vivo* genotoxicity assays that could be applied to the local target cells (41,50).

Secondary genotoxicity has been suggested to play an important role in the carcinogenic potential of fibrous nanomaterials, e.g. carbon nanotubes (51), and it may also be involved in the *in vivo* genotoxic response elicited by NFC in the present study. Macrophages and neutrophils are recruited to the site of particle deposition, as part of the normal innate inflammatory process, in response to an increase in the levels of pro-inflammatory cytokines, e.g. IL-1β (40) and generate reactive species (52) On the other hand, TNF-α has been suggested to stimulate the production of superoxide by monocytes and neutrophils, resulting in clastogenic effects (53). In this study, the number of macrophages in the BAL fluid showed a similar response as the induction of DNA damage in the lung cells, and our histological results demonstrated that NFC was present in the cytoplasm of macrophages. In addition, there was also a significant linear increase in the number of neutrophils and in the mRNA expression levels of IL-1β and TNF-α with the dose. However, the protein levels of both cytokines remained unaffected at the 24-h time point studied. Therefore, it is difficult to conclude whether these events are correlated.

In general, the genotoxic and inflammatory responses observed in the present study with NFC correspond with the known pulmonary toxicity previously reported for 'conventional' cellulose fibres (12–16). As the present study was based on an acute experiment, with sampling 24 h after a single pharyngeal aspiration of NFC, conclusions are limited to this short post-exposure time. A key question in the risk assessment of NFC is whether the inflammatory and genotoxic responses were transient or could persist for a longer time. The comet assay depicts primary DNA damage that is subject to repair, and is therefore short-lived, except for a small portion of damage that may turn into gene and chromosomal mutations due to errors in DNA repair and replication. However, if the conditions resulting in DNA damage prevail for a longer time, the probability of mutations accumulating will increase, which may contribute to cancer risk.

Conventional cellulose fibres have been described to have longer-term toxic effects in the lungs, which has been attributed to the low clearance and long persistence of cellulose (13). Granulomatous inflammation and fibrotic lesions caused by cellulose fibres were still present one year after a single intratracheal (2 mg/rat) deposition (16). On the other hand, inhalation experiments with rats indicated that thermo-mechanically processed wood cellulose fibres of various sizes caused a marked but transient inflammatory response, which did not progress after a recovery period of 28 days (13). Also nanocelluloses can be expected to be biopersistent. Exposure of different types of NFC and CNC to artificial lung airway lining fluid for up to 7 days and alveolar macrophage phagolysosomal fluid for up to 9 months suggested that cellulose nanomaterial is biodurable in the human lungs (54). In fact, 3 months post repeated CNC exposure, giant alveolar macrophages—which are recognised as the pathological hallmark of granulomatous diseases—were found in mice lungs (33).

Last but not least, the possible role of microbial contamination cannot be ruled out. Although the biocide was added immediately after the synthesis of our NFC to prevent microbial growth, some contamination could still have existed, contributing to the inflammatory effect.

In summary, our study showed that NFC administrated by pharyngeal aspiration caused an acute inflammatory response and DNA damage in murine lungs. Although the short post-exposure time (24 h) did not allow us to determine whether these responses were transient

or could persist for a longer time, the existing evidence on the low clearance and biopersistence of cellulose fibres rise concerns on their toxic hazards which need to be further assessed by longer-term studies.

Funding

This work was supported by European Commission under grant agreement FP7-228802 (SUNPAP).

Acknowledgements

We would like to thank Dr. D. Lison, Université catholique de Louvain (Belgium), for kindly providing us with tungsten carbide-cobalt mixture. Sandra Tapin-Lingua (Institut Technologique FCBA) and Sauli Savukoski (Finnish Institute of Occupational Health) are acknowledged for their excellent technical assistance in the production of the NFC and the histological preparations, respectively. The authors thank the NanoBio-ICMG Platform (Grenoble, France) for granting access to the electron microscopy facility for NFC characterisation by TEM.

Conflict of interest statement: None declared.

References

1. Siró, I. and Plackett, D. (2010) Microfibrillated cellulose and new nanocomposite materials: a review. *Cellulose*, 17, 459–494.
2. Klemm, D., Kramer, F., Moritz, S., Lindström, T., Ankerfors, M., Gray, D. and Dorris, A. (2011) Nanocelluloses: a new family of nature-based materials. *Angew. Chem. Int. Ed. Engl.*, 50, 5438–5466.
3. Lin, N. and Dufresne, A. (2014) Nanocellulose in biomedicine: Current status and future prospect. *Eur. Polym. J.*, 59, 302–325.
4. de Lima, R., Oliveira Feitosa, L., Rodrigues Maruyama, C., *et al.* (2012) Evaluation of the genotoxicity of cellulose nanofibers. *Int. J. Nanomed.*, 7, 3555–3565.
5. Hua, K., Ålander, E., Lindström, T., Mihranyan, A., Strømme, M. and Ferraz, N. (2015) Surface Chemistry of Nanocellulose Fibers Directs Monocyte/Macrophage Response. *Biomacromolecules*, 16, 2787–2795.
6. Lavoine, N., Desloges, I., Dufresne, A. and Bras, J. (2012) Microfibrillated cellulose - its barrier properties and applications in cellulosic materials: a review. *Carbohydr. Polym.*, 90, 735–764.
7. Vartiainen, J., Pohler, T., Sirola, K., *et al.* (2011) Health and environmental safety aspects of friction grinding and spray drying of microfibrillated cellulose. *Cellulose*, 18, 775–786.
8. Grosse, Y., Loomis, D., Guyton, K. Z., *et al.*; International Agency for Research on Cancer Monograph Working Group. (2014) Carcinogenicity of fluoro-edenite, silicon carbide fibres and whiskers, and carbon nanotubes. *Lancet. Oncol.*, 15, 1427–1428.
9. Knudsen, K. B., Kofoed, C., Espersen, R., *et al.* (2015) Visualization of Nanofibrillar Cellulose in Biological Tissues Using a Biotinylated Carbohydrate Binding Module of β-1,4-Glycanase. *Chem. Res. Toxicol.*, 28, 1627–1635.
10. Rylander, R., Schilling, R. S., Pickering, C. A., Rooke, G. B., Dempsey, A. N. and Jacobs, R. R. (1987) Effects after acute and chronic exposure to cotton dust: the Manchester criteria. *Br. J. Ind. Med.*, 44, 577–579.
11. International Agency for Research on Cancer (1995) Wood dust and formaldehyde. *IARC Monogr. Eval. Carcinog. Risks Hum.*, 62, 35–215.
12. Cullen, R. T., Miller, B. G., Clark, S. and Davis, J. M. (2002) Tumorigenicity of cellulose fibers injected into the rat peritoneal cavity. *Inhal. Toxicol.*, 14, 685–703.
13. Cullen, R. T., Miller, B. G., Jones, A. D. and Davis, J. M. G. (2002b) Toxicity of cellulose fibres. *Ann. Occup. Hyg.*, 46, 81–84.
14. Tátrai, E., Brozik, M., Adamis, Z., Merétey, K. and Ungváry, G. (1996) In vivo pulmonary toxicity of cellulose in rats. *J. Appl. Toxicol.*, 16, 129–135.
15. Adamis, Z., Tátrai, E., Honma, K. and Ungváry, G. (1997) In vitro and in vivo assessment of the pulmonary toxicity of cellulose. *J. Appl. Toxicol.*, 17, 137–141.
16. Muhle, H., Ernst, H. and Bellmann, B. (1997) Investigation of the durability of cellulose fibres in rat lungs. *Ann. Occup. Hyg.*, 41, 184–188.
17. Cullen, R. T., Searl, A., Miller, B. G., Davis, J. M. and Jones, A. D. (2000) Pulmonary and intraperitoneal inflammation induced by cellulose fibres. *J. Appl. Toxicol.*, 20, 49–60.
18. Schmitt, D. F., Frankos, V. H., Westland, J. and Zoetis, T. (1991) Toxicologic evaluation of Cellulon™ fiber; genotoxicity, pyrogenicity, acute and subchronic toxicity. *J. Am. Col. Toxicol.*, 10, 541–554.
19. Moreira, S., Silva, N. B., Almeida-Lima, J., Rocha, H. A., Medeiros, S. R., Alves, C. Jr and Gama, F. M. (2009) BC nanofibres: in vitro study of genotoxicity and cell proliferation. *Toxicol. Lett.*, 189, 235–241.
20. Jeong, S. I., Lee, S. E., Yang, H., Jin, Y.-H., Park, C.-S. and Park, Y. S. (2010) Toxicologic evaluation of bacterial synthesized cellulose in endothelial cells and animals. *Mol. Cell. Toxicol.*, 6, 373–380.
21. Kovacs, T., Naish, V., O'Connor, B., Blaise, C., Gagné, F., Hall, L., Trudeau, V. and Martel, P. (2010) An ecotoxicological characterization of nanocrystalline cellulose (NCC). *Nanotoxicology*, 4, 255–270.
22. Pitkänen, M., Kangas, H., Laitinen, O., Sneck, A., Lahtinen, P., Peresin, M. S. and Niinimäki, J. (2014) Characteristics and safety of nano-sized cellulose fibrils. *Cellulose*, 21, 3871–3886.
23. Alexandrescu, L., Syverud, K., Gatti, A. and Chinga-Carrasco, G. (2013) Cytotoxicity tests of cellulose nanofibril-based structures. *Cellulose*, 20, 1765–1775.
24. Bhattacharya, M., Malinen, M. M., Lauren, P., *et al.* (2012) Nanofibrillar cellulose hydrogel promotes three-dimensional liver cell culture. *J. Control. Release*, 164, 291–298.
25. Saska, S., Scarel-Caminaga, R. M., Teixeira, L. N., *et al.* (2012) Characterization and in vitro evaluation of bacterial cellulose membranes functionalized with osteogenic growth peptide for bone tissue engineering. *J. Mater. Sci. Mater. Med.*, 23, 2253–2266.
26. Lin, W. C., Lien, C. C., Yeh, H. J., Yu, C. M. and Hsu, S. H. (2013) Bacterial cellulose and bacterial cellulose-chitosan membranes for wound dressing applications. *Carbohydr. Polym.*, 94, 603–611.
27. Hua, K., Carlsson, D. O., Ålander, E., Lindstrom, T., Strømme, M., Mihranyan, A. and Ferraz, N. (2014) Translational study between structure and biological response of nanocellulose from wood and green algae. *RSC Adv.*, 4, 2892–2903.
28. Scarel-Caminaga, R. M., Saska, S., Franchi, *et al.* (2014) Nanocomposites based on bacterial cellulose in combination with osteogenic growth peptide for bone repair: cytotoxic, genotoxic and mutagenic evaluations. *J. Appl. Biol. Biotechnol.*, 2, 001–008.
29. Oliveira Barud, H. G., Barud, H. d. a. S., Cavicchioli, M., *et al.* (2015) Preparation and characterization of a bacterial cellulose/silk fibroin sponge scaffold for tissue regeneration. *Carbohydr. Polym.*, 128, 41–51.
30. Clift, M. J., Foster, E. J., Vanhecke, D., Studer, D., Wick, P., Gehr, P., Rothen-Rutishauser, B. and Weder, C. (2011) Investigating the interaction of cellulose nanofibers derived from cotton with a sophisticated 3D human lung cell coculture. *Biomacromolecules*, 12, 3666–3673.
31. Catalán, J., Ilves, M., Järventaus, H., Hannukainen, K. S., Kontturi, E., Vanhala, E., Alenius, H., Savolainen, K. M. and Norppa, H. (2015) Genotoxic and immunotoxic effects of cellulose nanocrystals in vitro. *Environ. Mol. Mutagen.*, 56, 171–182.
32. Yanamala, N., Farcas, M. T., Hatfield, M. K., Kisin, E. R., Kagan, V. E., Geraci, C. L. and Shvedova, A. A. (2014) In Vivo Evaluation of the Pulmonary Toxicity of Cellulose Nanocrystals: A Renewable and Sustainable Nanomaterial of the Future. *ACS Sustain. Chem. Eng.*, 2, 1691–1698.
33. Shvedova, A. A., Kisin, E. R., Yanamala, N., *et al.* (2016) Gender differences in murine pulmonary responses elicited by cellulose nanocrystals. *Part. Fibre Toxicol.*, 13, 28.
34. SCAN-CM 65:02 (2002) *Total acidic group content. Conductometric titration method*. Scandinavian Paper, Pulp and Board Testing Committee, Stockholm.
35. Lahtinen, P., Liukkonen, S., Pere, J., Sneck, A. and Kangas, H. (2014) A comparative study of fibrillated fibers from different mechanical and chemical pulps. *BioResources*, 9, 2115–2127.
36. Shvedova, A. A., Yanamala, N., Kisin, E. R., *et al.* (2014) Long-term effects of carbon containing engineered nanomaterials and asbestos in the lung:

one year postexposure comparisons. *Am. J. Physiol. Lung Cell. Mol. Physiol.*, 306, L170–L182.
37. Porter, D. W., Hubbs, A. F., Mercer, R. R., *et al.* (2010) Mouse pulmonary dose- and time course-responses induced by exposure to multi-walled carbon nanotubes. *Toxicology*, 269, 136–147.
38. Catalán, J., Suhonen, S., Huk, A. and Dusinska, M. (2014) Analysis of nanoparticle-induced DNA damage by the comet assay. In: Sierra LM, Gaivão I (eds) *Genotoxicity and DNA repair*. Humana Press, New York, pp. 241–268.
39. Lindberg, H. K., Falck, G. C., Singh, R., *et al.* (2013) Genotoxicity of short single-wall and multi-wall carbon nanotubes in human bronchial epithelial and mesothelial cells in vitro. *Toxicology*, 313, 24–37.
40. Rydman, E. M., Ilves, M., Vanhala, E., *et al.* (2015) A single aspiration of rod-like carbon nanotubes induces asbestos-like pulmonary inflammation mediated in part by the IL-1 receptor. *Toxicol. Sci.*, 147, 140–155.
41. Catalán, J., Siivola, K. M., Nymark, P., *et al.* (2016) *In vitro* and *in vivo* genotoxic effects of straight *versus* tangled multi-walled carbon nanotubes. *Nanotoxicology*, 26, 1–13.
42. OECD. (2014a) *Test Guideline 489, In Vivo Mammalian Alkaline Comet Assay*. Organization for Economic Cooperation and Development, Paris.
43. Lovell, D. P. and Omori, T. (2008) Statistical issues in the use of the comet assay. *Mutagenesis*, 23, 171–182.
44. OECD. (2014b) *Test Guideline 474, Mammalian Erythrocyte Micronucleus Test*. Organization for Economic Cooperation and Development, Paris.
45. Tanaka, A., Seppänen, V., Houni, J., Sneck, A. and Pirkonen, P. (2012) Nanocellulose characterization with mechanical fractionation. *Nordic Pulp Paper*, 27, 689–694.
46. Colic, M., Mihajlovic, D., Mathew, A., Naseri, N. and Kokol, V. (2015) Cytocompatibility and immunomodulatory properties of wood based nanofibrillated cellulose. *Cellulose*, 22, 763–778.
47. Kollar, P., Závalová, V., Hošek, J., Havelka, P., Sopuch, T., Karpíšek, M., Třetinová, D. and Suchý, P. Jr. (2011) Cytotoxicity and effects on inflammatory response of modified types of cellulose in macrophage-like THP-1 cells. *Int. Immunopharmacol.*, 11, 997–1001.
48. Magdolenova, Z., Collins, A., Kumar, A., Dhawan, A., Stone, V. and Dusinska, M. (2014) Mechanisms of genotoxicity. A review of in vitro and in vivo studies with engineered nanoparticles. *Nanotoxicology*, 8, 233–278.
49. Pinto, F. C., De-Oliveira, A. C., De-Carvalho, R. R., Gomes-Carneiro, M. R., Coelho, D. R., Lima, S. V., Paumgartten, F. J. and Aguiar, J. L. (2016) Acute toxicity, cytotoxicity, genotoxicity and antigenotoxic effects of a cellulosic exopolysaccharide obtained from sugarcane molasses. *Carbohydr. Polym.*, 137, 556–560.
50. Alenius, H., Catalán, J., Lindberg, H., Norppa, H., Palomäki, J. and Savolainen, K. (2014) Nanomaterials and human health. In Vogel, U., Savolainen, K., Wu, Q., van Tongeren, M., Brouwer, D. and Berges, M. (eds.), *Handbook of Nanosafety - Measurement, Exposure and Toxicology*. Academic Press, Waltham, pp. 59–133.
51. Kato, T., Totsuka, Y., Ishino, K., *et al.* (2013) Genotoxicity of multi-walled carbon nanotubes in both in vitro and in vivo assay systems. *Nanotoxicology*, 7, 452–461.
52. Donaldson, K., Poland, Stockholm C. A. and Schins, R. P. (2010) Possible genotoxic mechanisms of nanoparticles: criteria for improved test strategies. *Nanotoxicology*, 4, 414–420.
53. Emerit, I. (2007) Clastogenic factors as potential biomarkers of increased superoxide production. *Biomark. Insights*, 2, 429–438.
54. Stefaniak, A. B., Seehra, M. S., Fix, N. R. and Leonard, S. S. (2014) Lung biodurability and free radical production of cellulose nanomaterials. *Inhal. Toxicol.*, 26, 733–749.